# Dielectric Properties of Wood from 2 to 3 GHz

**Article** *in* Journal of Microwave Power and Electromagnetic Energy · February 2000

DOI: 10.1080/08327823.2000.11688430 · Source: PubMed



**4 authors**, including:

Roberto Olmi
Italian National Research Council


Cristiano Riminesi
Italian National Research Council

# Dielectric Properties of Wood From 2 to 3 GHz

**R. Olmi, M. Bini, A. Ignesti and C. Riminesi**

*Many applications of microwave energy to wooden materials have been developed in the last few decades, both for treatment and for diagnostic purposes. All these applications require a reliable estimation of the permittivity of the wood species of interest, which is the physical parameter of crucial importance in the absorption of electromagnetic energy. This paper presents results obtained in the dielectric characterization of five wood species in the frequency range from 2 to 3 GHz, including the ISM frequency of 2.45 GHz. Permittivity was measured by an open-ended coaxial-line probe of new design on wood samples conditioned at several moisture levels. The influence of the natural variability of wood characteristics on the measured permittivity was also investigated by a suitable experimental setup consisting of a poplar table including both sapwood and heartwood regions. Finally, a theoretical discussion on the meaning of a scalar measurement on anisotropic dielectrics is conducted in terms of an isotropic-equivalent permittivity, which is related to the permittivity tensor of the dielectric material.*

**Key Words:** Wood permittivity, anisotropic permittivity, dielectric properties

*ABOUT THE AUTHORS:*
R. Olmi, M. Bini, A. Ignesti and C. Riminesi are affiliated with IROE-CNR, Via Panciatichi 64, Firenze, Italy.



Several applications involving the interaction between electromagnetic (EM) energy and wooden materials demand accurate knowledge of the complex permittivity of different wood species over several frequency ranges [Antti and Torgovnikov, 1995, Bini et al., 1997a, Eskelinen and Harju, 1998, Franchois et al., 1998].

A knowledge of the dielectric characteristics of woods in different moisture conditions is required, for example, in the study of wood heating to quantify the interaction between the EM power and wood. That is actually the problem the authors have been faced with when studying the feasibility of the microwave disinfestation of artistic painted boards infested with woodworms [Bini et al., 1997b].

This paper reports the dielectric characteristics of five species of wood: Sylvester Pine, Poplar, Chestnut, Oak and Walnut. The measurements have been conducted in the frequency range from 2 to 3 GHz, centered around the ISM 2.45-GHz frequency used for microwave heating, on wood samples conditioned at various moisture levels from 0% (oven-dry wood) to about 30%, dry basis.

## Materials and Methods

Wood is an anisotropic dielectric which, greatly simplifying the physical reality, can be considered as a triaxial crystal, with three different principle axes related to the wood grain [Torgovnikov, 1993].

A thorough dielectric characterization of wood should therefore obtain the three complex components of a diagonal tensor of rank three. This is a very difficult task, especially when a non-destructive measurement is needed (e.g. when the material cannot be cut or damaged), and it is often a poorly defined task, because the direction of the wood grain changes from point to point making the permittivity tensor quite an aleatory quantity.

Fortunately, in several applications (e.g. for heating purposes or for determination of the moisture content) the knowledge of the permittivity tensor is not essential, while the estimate of an average complex permittivity is what is needed to quantify the EM interaction.

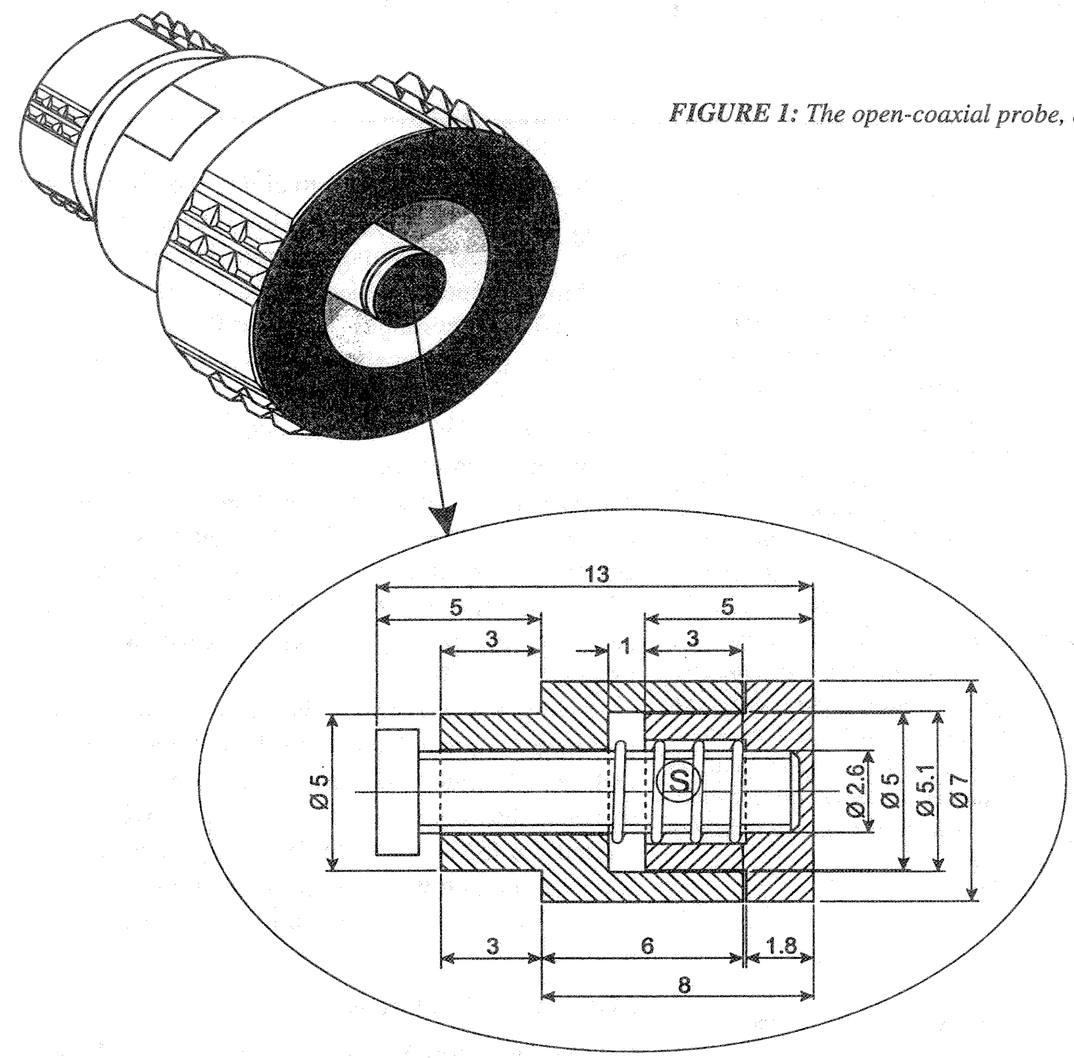


*FIGURE 1: The open-coaxial probe, dimensions in mm.*

### *The Measurement System*

The dielectric characteristics have been obtained by reflection measurements, with an open-coaxial probe specifically designed for measuring the permittivity of hard solid materials. The coaxial probe, shown in Figure 1, have been made by modifying a commercial connector used in power applications (BN293900). The probe consists of a transition from a standard N connector to one having diameters of 7 and 16 mm, respectively, for the inner and outer conductor. On the 7/16 side, the two conductors of the coaxial line have an air dielectric to minimize the error due to the presence of air gaps at the surface of the material under measurement. Moreover, the inner conductor has been lengthened by a section provided with a sliding end, maintained on axis with the central conductor by a screw and pushed out of the aperture plane by a steel spring. The mobile part ensures a good and easy contact between the probe and the dielectric under measurement, dramatically reducing the air gaps and allowing a highly reliable measurement. Details about the probe and the measurement system can be found elsewhere [Olmi et al., 2000].

The performance of the system has been verified on several solid materials of well-known dielectric characteristics (e.g. Teflon, Rexolite, several ceramics), in the frequency range from 2 to 3 GHz and for dielectric constants ($\varepsilon'$) between 2 and 12. The average accuracy is about $\pm 5\%$ for $\varepsilon'$ and $\pm 2 \cdot 10^{-3}$ for the loss tangent (tan $\delta$). The method is very reliable and measurements are highly reproducible, as verified by performing measurements on the same materials at different times, in different positions and after independent calibrations.

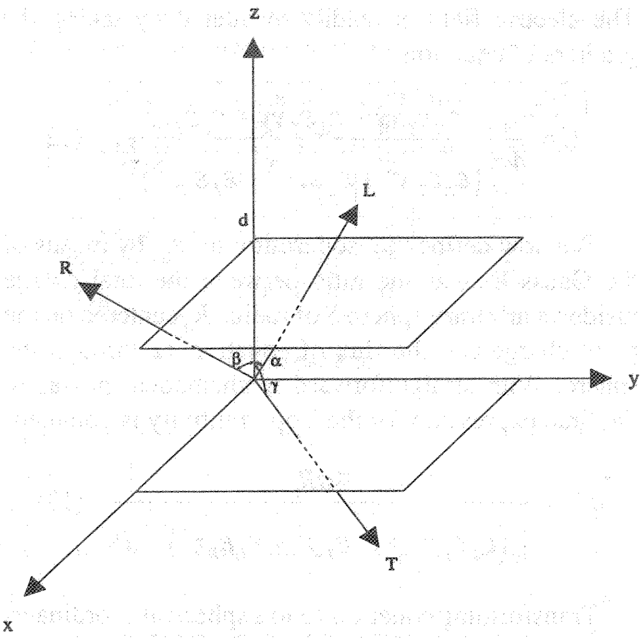


*FIGURE 2: Parallel-plate capacitor.*

### *Isotropic-Equivalent Dielectric Constant*

When measuring the complex permittivity of an anisotropic medium by means of a probe with a particular symmetry (as the open-ended coaxial probe), such that the electric field which "probes" the material cannot be directed along any of the principal axes of the dielectric, what we actually measure is an *isotropic equivalent* or *isopermittivity*. The isopermittivity must be related to the permitivity tensor, to understand what we are going to measure with an intrinsically isotropic device.

A simple qualitative reasoning, based on symmetry considerations [Smythe, 1968] would suggest that the measured isopermittivity is an average of the components of the tensor. Expressing the permittivity tensor with respect to the principal axes L, R and T (with reference to [Torgovnikov, 1993]), and limiting ourselves to the case of an ideal dielectric (no losses):

$$\underline{\underline{\varepsilon}} = \begin{pmatrix} \varepsilon_L & 0 & 0 \\ 0 & \varepsilon_R & 0 \\ 0 & 0 & \varepsilon_T \end{pmatrix} \qquad (1)$$

the first-impression isopermittivity is therefore:

$$\varepsilon_{iso} = \frac{1}{3}\left(\varepsilon_L + \varepsilon_R + \varepsilon_T\right). \qquad (2)$$

### *The Parallel-Capacitor Model*

Let us consider an ideal parallel-plate capacitor filled with an anisotropic, homogeneous dielectric having the permittivity $\underline{\underline{\varepsilon}}$ given by equation 1.

Figure 2 shows the geometry of such a capacitor. The $\hat{z}$ unit vector (normal to the capacitor plates placed in z=0 and z=d) makes angles $\alpha$, $\beta$ and $\gamma$ with the dielectric principal axes L, R and T. The upper electrode (z=d) is taken at a potential V, while the lower one is at zero. From symmetry considerations, the equipotential surfaces are planes parallel to the capacitor plates (z=constant).

In the LRT system of coordinates, the potential is thus constant over planes of equation:

$$L\cos\alpha + R\cos\beta + T\cos\gamma = z \qquad (3)$$

and it is given by:

$$\phi(z) = \frac{V}{d}z = \frac{V}{d}\left(L\cos\alpha + R\cos\beta + T\cos\gamma\right). \qquad (4)$$

The electric displacement field between the plates is:

$$\underline{D} = -\underline{\underline{\varepsilon}}\nabla\phi = -\frac{V}{d}\left[\varepsilon_L\cos\alpha\hat{L} + \varepsilon_R\cos\beta\hat{R} + \varepsilon_T\cos\gamma\hat{T}\right]. \qquad (5)$$

An application of the Gauss law to a cylinder along $\hat{z}$ having unitary base surfaces on the planes z=0 and z=d allows the computation of the capacitance per unit surface $C_u$:

$$C_u = \frac{1}{V}\left|\underline{D}\cdot\hat{z}\right| = \frac{1}{V}\left|\underline{D}\cdot\left(\cos\alpha\hat{L} + \cos\beta\hat{R} + \cos\gamma\hat{T}\right)\right| = \frac{\varepsilon_L\cos^2\alpha + \varepsilon_R\cos^2\beta + \varepsilon_T\cos^2\gamma}{d} \qquad (6)$$

By comparing equation 6 with the capacitance per unit surface of a capacitor filled with an isotropic dielectric $\varepsilon_{iso}$ the latter is computed as:

$$\varepsilon_{iso} = \varepsilon_L\cos^2\alpha + \varepsilon_R\cos^2\beta + \varepsilon_T\cos^2\gamma \qquad (7)$$

### *The Charge Model*

The above derivation of the isopermittivity suffers for the peculiar geometry involved. In open-coaxial measurements the electric field in the probed material has a very complex configuration, and equation 7 cannot be rigorously applied.

A possible, simplified approach to the problem is the following. As a first approximation, the electric field produced by the open coaxial line in the material is a quasistatic one, and it is therefore closely connected to the charge distribution on the inner and outer electrodes at the coaxial aperture. It seems reasonable to gain knowledge on the effect of anisotropy by investigating the effect of anisotropy on a single point charge and then invoking the superposition principle to extend the results to the full, unknown charge distribution.

The potential in an anisotropic medium of permittivity $\underline{\underline{\varepsilon}}$ due to a point charge $q$ placed at $\hat{z}$ is found by solving the following equation:

$$\nabla \cdot \underline{\underline{\varepsilon}}\,\underline{E} = q\delta\left(\underline{r} - \underline{r_0}\right). \qquad (8)$$

Placing the charge at the origin of a Cartesian rectangular system of coordinates $(x,y,z)$ coincident with the dielectric axes $(L,R,T)$, the above equation 8 becomes the Poisson equation for the electrostatic potential:

$$\varepsilon_L \frac{\partial^2 \phi}{\partial x^2} + \varepsilon_R \frac{\partial^2 \phi}{\partial y^2} + \varepsilon_T \frac{\partial^2 \phi}{\partial z^2} = -q\delta(x,y,z). \quad (9)$$

To solve equation 9, a useful coordinate transformation can be applied. If the following $\xi$, $\eta$ and $\zeta$ are respectively substituted for $x$, $y$ and $z$:

$$\xi = x / \sqrt{\varepsilon_L}$$
$$\eta = y / \sqrt{\varepsilon_R}$$
$$\zeta = z / \sqrt{\varepsilon_T}$$

Equation 9 becomes:

$$\frac{\partial^2 \phi}{\partial \xi^2} + \frac{\partial^2 \phi}{\partial \eta^2} + \frac{\partial^2 \phi}{\partial \zeta^2} = -q\delta(\xi,\eta,\zeta). \qquad (10)$$

Equation 10 is readily solved, as it refers to a point charge $q$ in a vacuum. The solution of equation 9 is therefore [Landau and Lifshits, 1995]:

$$\phi = \frac{q}{4\pi}\left(\varepsilon_R\varepsilon_T x^2 + \varepsilon_L\varepsilon_T y^2 + \varepsilon_L\varepsilon_R z^2\right). \qquad (11)$$

The electric field is readily evaluated by taking the gradient of equation 11:

$$\underline{E} = \frac{q}{4\pi} \frac{\varepsilon_R\varepsilon_T x\hat{x} + \varepsilon_L\varepsilon_T y\hat{y} + \varepsilon_L\varepsilon_R z\hat{z}}{\left(\varepsilon_R\varepsilon_T x^2 + \varepsilon_L\varepsilon_T y^2 + \varepsilon_L\varepsilon_R z^2\right)^{\frac{3}{2}}}. \qquad (12)$$

We now define the isopermittivity $\varepsilon_{iso}$ by means of the Gauss law, as the ratio between the total charge inside an arbitrary sphere $S$ of radius $R_0$ centered on the point charge and the flux of equation 12 through the sphere. With straightforward mathematical passages, the final expression for the isopermittivity is obtained:

$$\varepsilon_{iso} = \frac{4\pi R_0}{\int_S \left(\varepsilon_R\varepsilon_T x^2 + \varepsilon_L\varepsilon_T y^2 + \varepsilon_L\varepsilon_R z^2\right)^{-\frac{1}{2}} dS}. \qquad (13)$$

Transforming equation 13 to a spherical coordinates system $(R_0, \theta, \varphi)$ the final expression is computed as:

$$\varepsilon_{iso} = \frac{4\pi}{\int_0^{2\pi} d\varphi \int_0^{\pi} \sin\theta d\theta \left(\varepsilon_R\varepsilon_T \sin^2\theta\cos^2\varphi + \varepsilon_L\varepsilon_T \sin^2\vartheta\sin^2\varphi + \varepsilon_L\varepsilon_R \cos^2\varphi\right)^{-\frac{1}{2}}}. \qquad (14)$$

*Numerical Data*

We apply equations 2, 7 and 14 to permittivity data reported by Skaar [1988] for dry wood as a function of grain orientation. In the reported case the permittivity tensor is:

$$\underline{\underline{\varepsilon}} = \begin{pmatrix} 2.6 & 0 & 0 \\ 0 & 1.8 & 0 \\ 0 & 0 & 1.7 \end{pmatrix}$$

The isopermittivities computed by the three formulas are:
$\varepsilon_{iso}$=2.03 by equation 2
$\varepsilon_{iso}$=1.95 by equation 7, with $\alpha=\beta=\pi/3$ and $\gamma=\pi/4$
$\varepsilon_{iso}$=2.003 by equation 14

The $\varepsilon_{iso}$ computed by equation 7 obviously depends on the chosen direction cosines, ranging between 1.7 (for $\gamma$=0) and 2.6 (for $\alpha$=0).

As another example, consider a piece of Douglas fir wood at 20°C, with 15% moisture content, which has a permittivity $\varepsilon_L$=5, $\varepsilon_R \cong \varepsilon_T = 3$. In this case it can be

*TABLE 1: Relative humidity values in the conditioning chamber and corresponding wood equilibrium moisture contents.*

| Wood species | Relative Humidity, % (RH) | | | |
|---|---|---|---|---|
| | 30 | 55 | 90 | 98 |
| Chestnut | 7 | 12 | 22 | 27 |
| Walnut | 8 | 13 | 25 | 31 |
| Sylvester pine | 7 | 13 | 22 | 28 |
| Poplar | 7 | 10 | 27 | 34 |
| Oak | 6 | 12 | 21 | 26 |

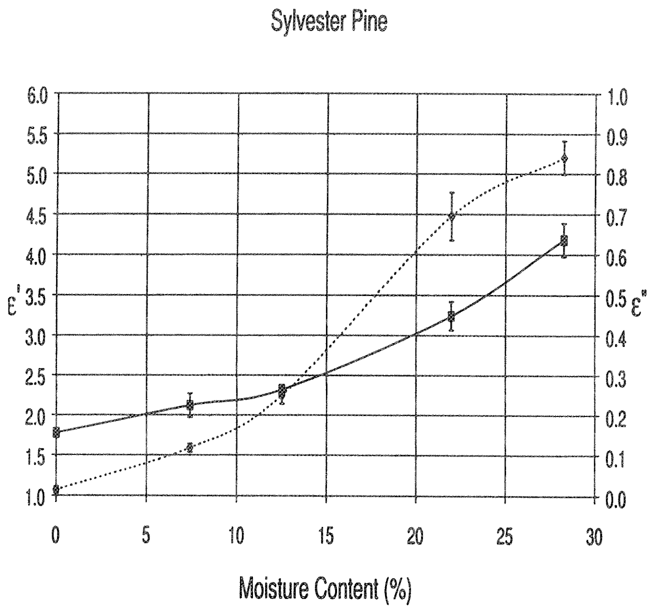


*FIGURE 3: Real part ε' (solid line) and imaginary part ε" (dotted line) of the permittivity of Sylvester pine as a function of moisture content at 2.45 GHz, ambient temperature (25°C).*

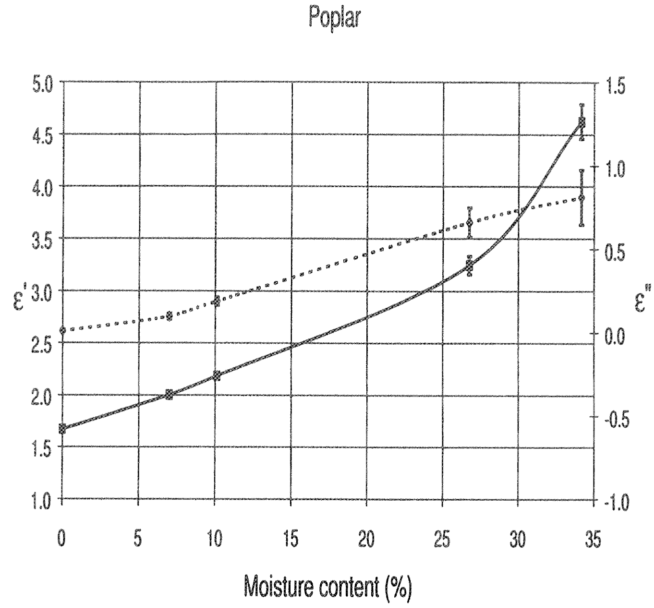


*FIGURE 4: Real part ε' (solid line) and imaginary part ε" (dotted line) of the permittivity of Poplar as a function of moisture content at 2.45 GHz, ambient temperature (25°C).*

computed $\varepsilon_{iso}$=3.6 by equation 14.

It can be concluded that, in the absence of any information about the orientation of the electric field with respect to the anisotropy axes of the dielectric, the measured quantity can be reasonably assumed to be an average of the components of the permittivity tensor and computed indifferently by means of equations 2 or 14.

## Results

Dielectric measurements have been conducted on five wood species (Sylvester pine, Poplar, Chestnut, Walnut and Oak) both as a function of frequency, around 2.45 GHz, and of moisture content (M). Four samples for each wood species were cut from different board sections — ranging from alburnum (sapwood) to duramen (heartwood) — and conditioned at various M levels. The size of the sample was 6x6x5 cm.

Apart from the 0% M, obtained by drying the samples at 103°C in a dry-air ventilated oven for several hours according to the procedure reported by Skaar [1988], all other Ms were obtained by conditioning the samples at different humidity levels in an airtight chamber. Table 1 shows the humidity levels and the corresponding Ms reached by the five wood species.

With reference to Table 1, the humidity levels were obtained by means of the following solutions: saturated solution of calcium chloride ($CaCl_2$) in water (RH=30%); natural ambient conditions (RH=55%); saturated solution of potassium nitrate ($KNO_3$) water-vapor saturated environment (RH=98%). Humidity and temperature were accurately controlled by means of a precision thermo-hygrometer (Rotronic Hygromer C94). For all samples, equilibrium conditions were reached in about 25 days.

Figures 3 to 7 show the complex isopermittivity of Sylvester pine, Poplar, Chestnut, Walnut and Oak as a function of M at 2.45 GHz. Figures 8 to 12 show the dielectric characteristics of the same wood species as a function of frequency. In all these figures solid and dotted lines respectively represent the dielectric constant and the dielectric loss. The smooth curves, con-

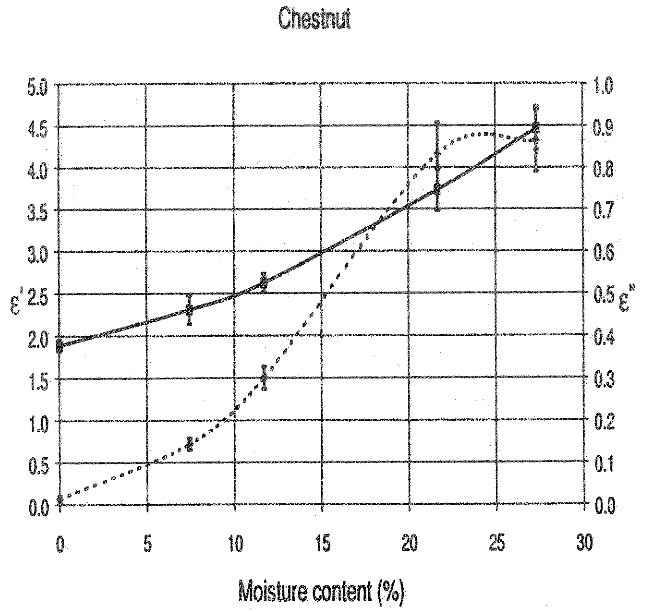


*FIGURE 5: Real part ε' (solid line) and imaginary part ε" (dotted line) of the permittivity of Chestnut as a function of moisture content at 2.45 GHz, ambient temperature (25°C).*

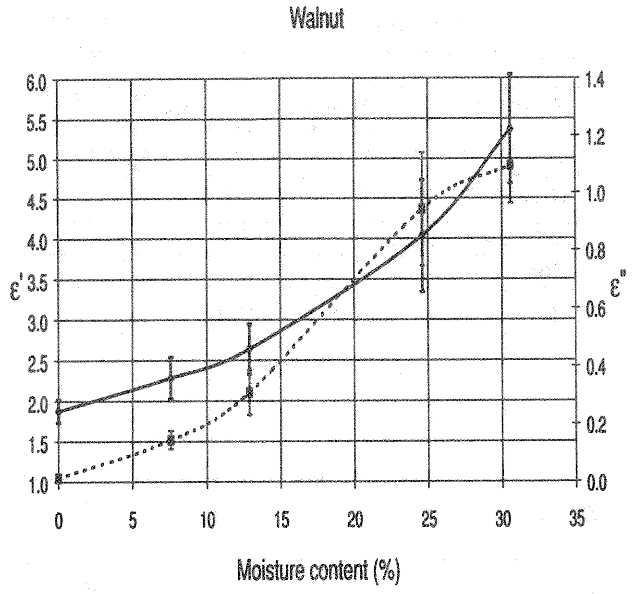


*FIGURE 6: Real part ε' (solid line) and imaginary part ε" (dotted line) of the permittivity of Walnut as a function of moisture content at 2.45 GHz, ambient temperature (25°C).*

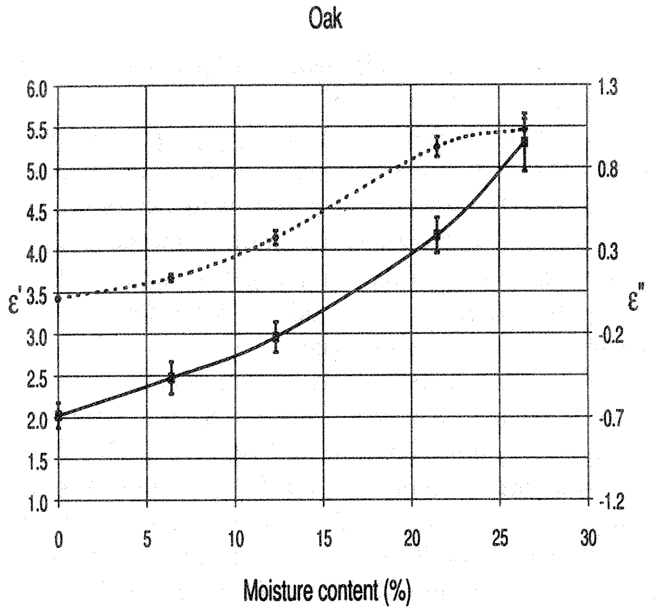


*FIGURE 7: Real part ε' (solid line) and imaginary part ε" (dotted line) of the permittivity of Oak as a function of moisture content at 2.45 GHz, ambient temperature (25°C).*

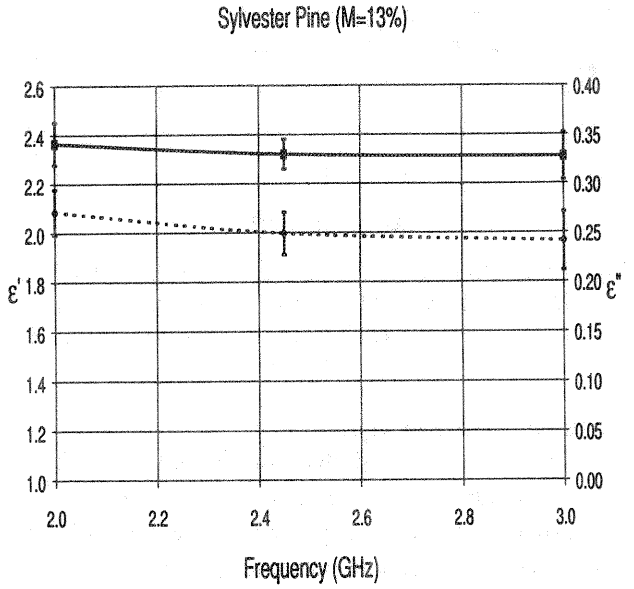


*FIGURE 8: Real part ε' (solid line) and imaginary part ε" (dotted line) of the permittivity of Sylvester pine as a function of frequency at 13% moisture content and ambient temperature (25°C).*

necting the experimental average points, have been produced by a spline-procedure.

### *Measurement Reproducibility and the Natural Variability of Wood*

Wood is an inhomogeneous material. In order to test both the natural variability of wood permittivity and the performances of the probe, a particular experiment has been designed and performed. A grid was drawn on a poplar table of size 21x21x5 cm, having 36 squares 3.5 cm on each side (to accommodate the dielectric probe). Three different materials can be recognized in the grid

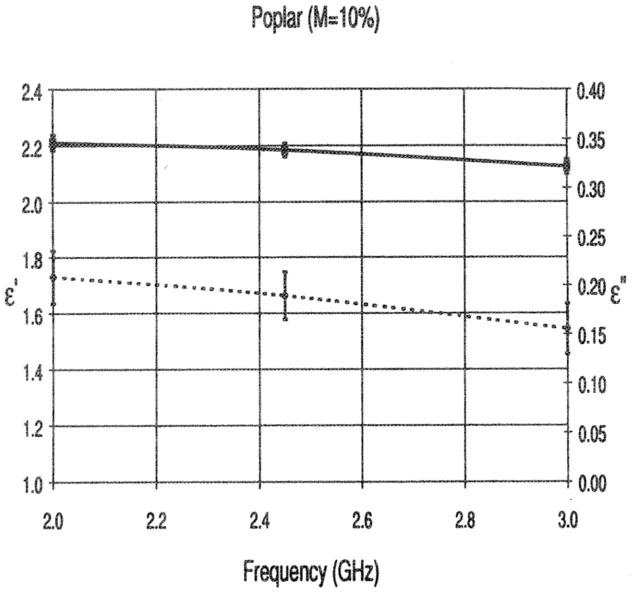


*FIGURE 9: Real part ε' (solid line) and imaginary part ε'' (dotted line) of the permittivity of Poplar as a function of frequency at 13% moisture content and ambient temperature (25°C).*

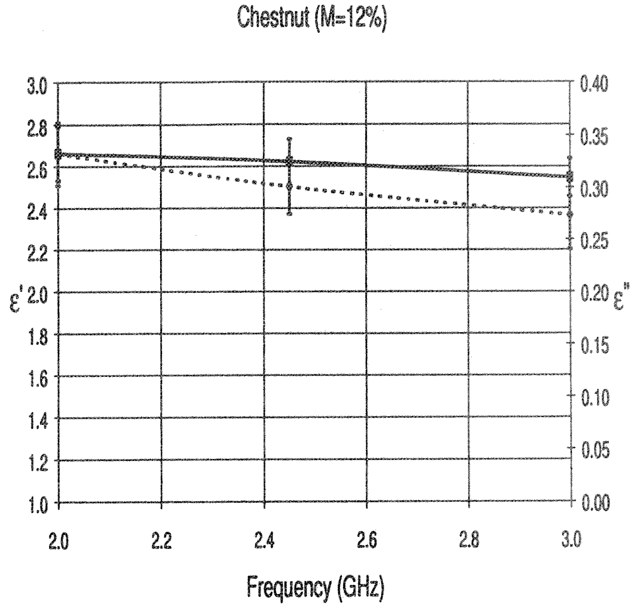


*FIGURE 10: Real part ε' (solid line) and imaginary part ε'' (dotted line) of the permittivity of Chestnut as a function of frequency at 13% moisture content and ambient temperature (25°C).*

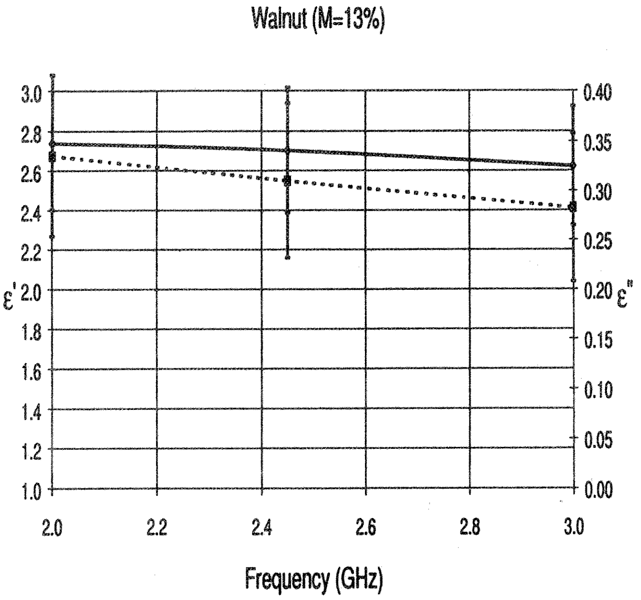


*FIGURE 11: Real part ε' (solid line) and imaginary part ε'' (dotted line) of the permittivity of Walnut as a function of frequency at 13% moisture content and ambient temperature (25°C).*

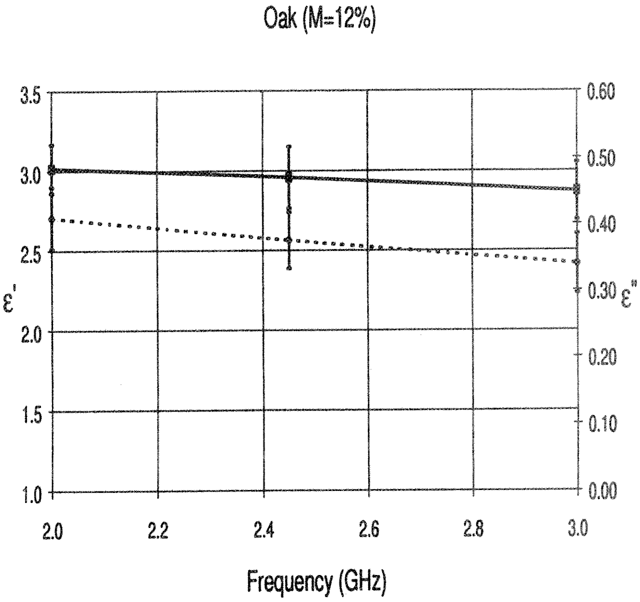


*FIGURE 12: Real part ε' (solid line) and imaginary part ε'' (dotted line) of the permittivity of Oak as a function of frequency at 13% moisture content and ambient temperature (25°C).*

(Figure 13): alburnum (9 squares), duramen (18 squares) and mixed (9 squares).

Three series of measurements were conducted at a frequency of 2.45 GHz on the 36 squares, for a total of 108 measurements. The three series of measurement were performed after independent calibrations of the system to test the reliability of measurement. The board was kept at ambient temperature (about 25°C) and ambient humidity (corresponding to an M between 10% and 13%).

Table 2 summarizes the measurement results. The fourth and sixth columns show that the standard devia-

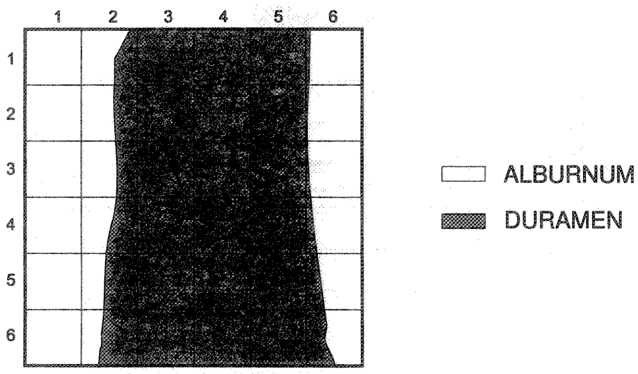


*FIGURE 13: The "poplar grid-system": a poplar board subdivided in 36 squares.*

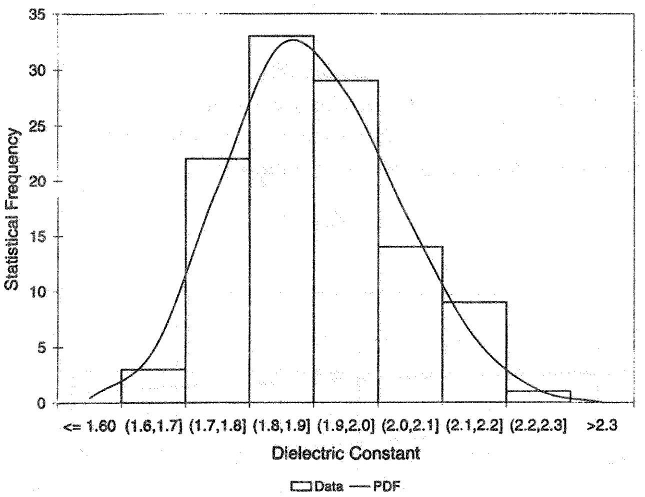


*FIGURE 14: Comparison between the statistical frequency of measured dielectric constant and its theoretical probability density function (PDF).*

tion is low both on the real part and on the imaginary part of permittivity. This variability is mainly due to the intrasquare diversity (i.e. to the different characteristics of squares of the same material type), confirming the good reproducibility and reliability of the measuring system.

It can be easily shown that the probability density distributions of both $\varepsilon'$ and $\varepsilon''$ are mixtures of three normal distributions pertaining to the three materials, weighted by their relative frequency of appearance in the grid system (see Appendix).

Figures 14 and 15 respectively compare the measured statistical frequencies of the dielectric constant and of the loss factor with the theoretical probability density. The real part of permittivity almost always belongs to an interval ranging ±10%, about 1.9. The imaginary part is more dispersed, ranging ± 20%, about 0.1.

*TABLE 2: Variability of the complex permittivity of a Poplar board.*

| Material | No. of squares | $\epsilon'$ | St.Dev.($\epsilon'$) | $\epsilon''$ | St.Dev.($\epsilon''$) |
|---|---|---|---|---|---|
| Alburnum | 9 | 1.84 | 0.084 | 0.12 | 0.009 |
| Mixed | 9 | 1.85 | 0.092 | 0.11 | 0.015 |
| Duramen | 18 | 1.98 | 0.107 | 0.09 | 0.010 |

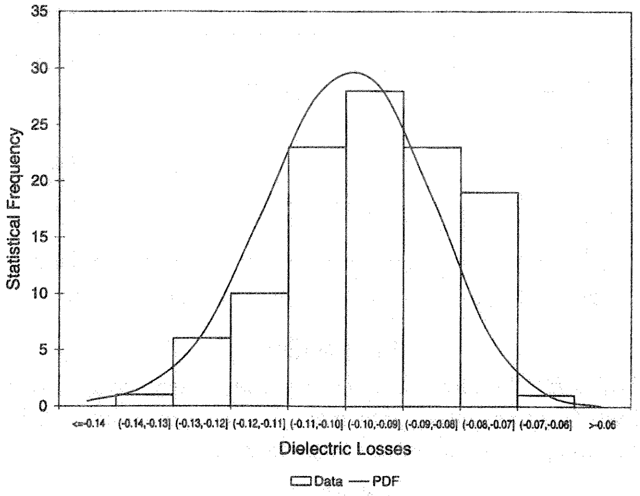


*FIGURE 15: Comparison between the statistical frequency of measured dielectric losses and its theoretical probability density function (PDF).*

## Conclusions

The relation has been investigated between the permittivity tensor of wood and an isotropic-equivalent permittivity obtained by open-coaxial line measurements.

A new type of open-coaxial probe has been used, allowing precise and reliable dielectric measurements to be performed on hard, solid materials.

Five species of wood have been characterized in the frequency range from 2 to 3 GHz centered on the ISM frequency of 2.45 GHz, as a function of the moisture content.

An analysis of the effect on the dielectric properties of the natural variability of a widely used wood species (poplar) has also been performed, resulting in an estimate of the expected limits of variation for wood permittivity. The effect of natural variability has been described in terms of the probability density distributions for the real and imaginary part of permittivity, which were shown to consist in mixtures of three normal distribution pertaining to sapwood, heartwood and mixed material.

A theoretical discussion on the meaning of a scalar measurement on anisotropic dielectrics has been conducted by introducing the concept of isopermittivity, a scalar parameter related to the permittivity tensor of an anisotropic dielectric material. The isopermittivity is what a probe having a particular symmetry (as coaxial-line probes) actually measures. It has been theoretically demonstrated that isopermittivity simply coincides with an average among the components of the permittivity tensor, when no information is available about the orientation of the electric field with respect to the anisotropy axes.

## Appendix

Denoting by $n_a$, $n_m$ and $n_d$ respectively, the number of alburnum, mixed material and duramen squares in the grid system, and by $N_t$ the total number of squares, the corresponding probability of measuring alburnum, mixed material or duramen is $P(i)=n_i/N_t$, with i="a," "m" or "d."

Given a particular square "$Q_i$" of dielectric constant $\varepsilon_i'$, the probability for $\varepsilon'$ —conditioned to the choice of the "i" square — is assumed to be normal with mean $\varepsilon_i'$ and variance $s_i^2$.

$$p(\varepsilon'|i) = N(\varepsilon_i', s_i^2).$$

The probability of measuring a certain $\varepsilon'$ requires an integration of the "$Q_i$" parameter over all possible squares (a statistical procedure known as "marginalization"):

$$p(\varepsilon') = \int_i p(\varepsilon' Q_i)di = \int_i p(\varepsilon'|Q_i)P(Q_i)dQ_i = \sum_i p(\varepsilon'|Q_i)P(Q_i)$$

with the intregral extended to the three square types present on the grid, and the last passage coming from the discrete nature of the problem.

The probability of measuring an $\varepsilon'$ in a given range, say $[\varepsilon_1', \varepsilon_2']$,, is thus given by:

$$P(\varepsilon') = \int_{\varepsilon_1'}^{\varepsilon_2'} p(\varepsilon')d\varepsilon'$$

where the probability density p($\varepsilon'$) is given by:

$$p(\varepsilon') = \frac{n_a}{N_t} N(\varepsilon_a, s_a^2) + \frac{n_m}{N_t} N(\varepsilon_m, s_m^2) + \frac{n_d}{N_t} N(\varepsilon_d, s_d^2)$$

The probability density p($\varepsilon''$) can be obtained by a nearly identical procedure.

## References


Antti, A.L. and Torgovnikov, G. (1995), Microwave Heating of wood. Proc. 5th Internat. Conf. Microwave High Frequency Heating, pp. E3.1-E3.4.

Bini, M., Andreuccetti, D., Ignesti, A., Olmi, R., Priori, S. and Vanni, R. (1997a), Treatment planning in the microwave heating of painted wood boards. Proc. 6th Internat. Conf. Microwave High Frequency Heating, 631-364.

Bini, M., Andreuccetti, D., Ignesti, A., Olmi, R., Priori, S. and Vanni, R. (1997b), A portable microwave system for woodworm disinfestation of artistic painted boards. Journal of Microwave Power and Electromagn. Energy, 32: 180-187.

Eskelinen, P. and Harju, P. (1998), Characterizing wood by microwaves. IEEE AES Systems Magazine, February, pp. 34-35.

Franchois, A., Pineiro, Y. and Lang, R.H. (1998), Microwave permittivity measurements of two conifers. IEEE Trans. Geoscience and Remote Sensing, 36: 1384-1395.

Landau, L.D. and Lifshits, E.M. (1995), Electrodynamics of continuous media. Butterworth-Heinemann Publishers, London.

Olmi, R., Bini, M., Ignest., A. and Riminesi, C. (2000), Non-destructive permittivity measurements of solid materials. To be published in Measurement Science and Technology.

Skaar, C. (1988), Wood-Water Relations. Springer Verlag, Berlin.

Smythe, W.R., (1968), Static and Dynamic Electricity. McGraw-Hill Bood Company, New York.

Torgovnikov, G.I. (1993), Dielectric Properties of Wood and Wood-Based Materials. Springer Verlag, Berlin.